OFDM RoFSO Links with Relays Over Turbulence Channels and Nonzero Boresight Pointing Errors

George K. Varotsos, Hector E. Nistazakis, and George S. Tombras
Department of Electronics, Computers, Telecommunications and Control, Faculty of Physics, National and Kapodistrian University of Athens, Athens, 15784, Greece
e-mails: {georgevar; enistaz; gtombras}@phys.uoa.gr

Abstract —In the last few years, the radio on free space optics (RoFSO) technology that involves effective wireless transmissions of multiple radio frequency (RF) signals via free space optical (FSO) links, has drawn great research and commercial interest. However, its deployment suffers from atmospheric turbulence and pointing errors effects that strongly degrade the performance of such optical wireless links. In order to combat these impairments, in this work, we investigate the performance of various realistic RoFSO scenarios that may employ orthogonal frequency-division multiplexing (OFDM) scheme with Quadrature Amplitude Modulation (QAM) format and Decode and Forward (DF) relay node(s) over weak to strong turbulence channels emulated through the very accurate recently launched Malaga or *M*-distribution model along with the presence of various nonzero boresight pointing errors effects with different jitters for the elevation and the horizontal displacement modeled through the suitable Beckmann distribution. Under these conditions we extract closed-form mathematical expressions for the crucial performance metrics of the Outage Probability (OP) and the Average Bit Error Rate (ABER) of the examined RoFSO implementations with DF relays. Proper numerical results that are validated through the corresponding simulations are provided and demonstrate the accuracy of our extracted expressions along with the usefulness of serial DF relay-assisted multi-hop configurations as an effective method to broaden the coverage of the optical wireless links.

Index Terms—Radio on Free space Optical (RoFSO) technology; *M*alaga-distribution; Decode and Forward (DF) relays; Nonzero boresight pointing errors; Orthogonal Frequency Division Multiplexing (OFDM); Quadrature Amplitude Modulation (QAM).

I. Introduction

A. RoF and RoFSO Techniques

Owing to the increasing demand for transferring higher data rates at a higher security level, the transmission of RF signals through optical wavelengths has attained a lot of commercial and research interest recently. In this respect, both radio over fiber (RoF) and RoFSO technologies provide the means to accommodate these growing requirements.

Transmission of RF signals by means of optical fiber links, has been utilized for many years as a cost-effective and high-capacity solution to facilitate the wireless access [1]. Since its first demonstration for cordless or mobile telephone service in 1990, [2], the RoF technology has been developed to provide high transmission capacity, significant mobility and flexibility, as well as economic advantage due to its broad bandwidth and low attenuation characteristics. In addition, RoF systems allow multi-operator multi-service operation, and dynamic resource allocation. These potentials have made it suitable for wide range of applications including last mile solutions, extension of existing radio coverage and capacity, and backhaul. In RoF implementation, to distribute the RF signals from central station to remote stations, RF signals are placed on optical carriers and transmitted over high capacity optical fiber cables [3]-[6]. However, RoF implementation is dependent on availability of installed optical fiber cables [7].

Therefore, in the absence of fiber infrastructure (for example across a river, a very busy street, rail tracks or where right of way is not available or too expensive to pursue), RoFSO is an attractive data bridge in such instances, [7], [8]. Similar to RoF technique, it has been demonstrated recently that the RF signals can be transmitted by a line-of-sight (LOS) relatively short FSO link, using the so-called RoFSO scheme, [7], [9], [10]. In fact, by modulating RF signals on optical carriers for transmission over the free space, RoFSO systems have the same advantages and drawbacks with FSO links. More specifically, by increasing the carrier frequency from RF to that of optical waves through RoFSO technique, it is feasible to increase the information capacity by many orders of magnitude and even at a higher security level due to the fact that the information data is transmitted through a very narrow optical beam, which is very difficult to detect and interfere, [8], [11]-[17].

Other benefits of FSO propagation that also harvest RoFSO transmissions include the immunity to multipath dispersion and electromagnetic interference, the operation with lower power consumption in the unlicensed optical spectrum, the flexibility for deployment and redeployment and lower overall installation and operational costs compared to conventional radio links and fiber optics, [8], [14], [16], [18]-[22]. In view of these nice characteristics features mentioned above, RoFSO can be used either as an effective alternative or

Manuscript received July 20, 2017; revised November 20, 2017.
doi:10.12720/jcm.12.12.644-660

complementary to the optical fiber network as a high capacity wireless backhaul technology for cellular networks, [1], [9], [23]-[25]. Moreover, new generation of FSO systems utilize seamless connection of free-space beam to optical fiber and therefore eliminating the necessity of converting the transmitted signal from optical-to-electrical or vice versa, [26].

This kind of FSO system realizes a bandwidth and protocol transparent system, which can be easily adapted for the transmission of RF signals through RoFSO communication, [27]. RoFSO technology has also been suggested to provide inexpensive, secure, short-range wireless transport for WiMAX (Worldwide Interoperability for Microwave Access) as reported in [28]-[32]. Additionally, another point in favor of RoFSO is that while the data rate over fiber is limited by its dispersion characteristics [33], [34] the dispersion due to atmosphere is shown to be much weaker or even negligible for short propagation distances [16], [35]-[37]. Finally, via RoFSO technology it is possible to simultaneously transmit multiple RF signals comprising heterogeneous wireless services over FSO links using wavelength-division multiplexing technology, while it can be also applied as a universal platform for enabling seamless convergence of fiber and free-space optical communication networks, thus extending broadband connectivity to underserved areas [7].

B. Challenges of RoFSO Technology Development

However, the widespread deployment of RoFSO is hampered by several performance-degrading factors that mainly arise from the variable characteristics of the atmospheric FSO channel. Effects of fog, rain, atmospheric gases and aerosols result in beam attenuation because of photon absorption and scattering [38], [39]. It is notable that similarly to our viewing of distant object the optical transmission is most impaired by fog i.e. more than 30dB/km, because the fog aerosols have a comparable size as the used optical wavelengths, causing much scattering of the laser energy as the fog gets thicker [40]-[42]. Nevertheless, both absorption and scattering are deterministic effects that are extensively studied, especially under fog conditions [17], [43] and thus they are not treated in this paper.

Even in clear weather conditions a major impairment over FSO and RoFSO propagation is the very complex and random atmospheric turbulence effect which takes place because of the inhomogeneities of both temperature and pressure in the atmospheric channel and causes the so-called scintillation effect that results in rapid fluctuations of the irradiance of the optical signal at the receiver's side, degrading strongly the communication system's performance, [23], [36], [39], [44]-[46]. Thus, in order to emulate these turbulence-induced irradiance scintillations, accurate turbulence distribution models are required according to turbulence strength. In early works on optical wireless communications the lognormal model has been widely used [45], [47]-[52]. However, this model has been proved to be valid only for weak turbulence conditions. Alternatively, the I-K distribution model [36], [53]-[55] and the Gamma model [16], [56]-[58] can be also used in the weak turbulence regime. Under strong turbulence conditions it has been shown that K distribution is in a good agreement with experimental results [59]-[62], while for saturated turbulence conditions the negative exponential distribution has been proved to be suitable [23], [50], [63]-[68].

A very accurate turbulence-induced fading channel model for FSO systems is the Gamma-Gamma distribution proposed by Al-Habash *et al*. in [69] and has a very good agreement with measurement data for a wide range of weak to strong turbulence conditions. This tractable mathematical model for atmospheric turbulence is based on the modified Rytov theory that was introduced by the same authors in [70], while it is notable that includes both the negative exponential and K distribution models as its marginal cases. Representative examples of the wide use of Gamma-Gamma model in optical wireless communications can be found in [9], [16], [23], [36], [71]-[78]. Nevertheless, the distribution model that leads to closed-form and mathematically tractable expressions under all turbulence regimes, unifying most of the well-known proposed statistical models for turbulence-induced irradiance fluctuations is the recently-launched *M-alaga* distribution model that was first suggested by Navas *et al*. in [79]. Indeed, lognormal, negative exponential, gamma, K and even gamma-gamma model are proved to be special cases of *M*-alaga distribution, [79].

In this context, *M*-(alaga) distribution is gaining popularity in scientific bibliography recently, as it can be realized in [24], [80]-[84] and it will be also used to model the irradiance scintillations in the current work. Additionally, Ansari et al. derived in [81] very useful unified formulas and asymptotic expressions for the most important performance metrics of an FSO link operating over *M*-alaga turbulence, such as the outage probability, the error rate of a variety of modulation schemes and the ergodic capacity. Furthermore, Sandalidis *et al*. in [85] proposed the mixture Gamma distribution model as an accurate approximation of the turbulence effect, mainly in an attempt to simplify the expressions of Gamma-Gamma and *M*-(alaga) functions, [85], [86].

Another significant concern of FSO and RoFSO development is the unavoidable presence of pointing errors due to building sway, namely misalignments between the transmit and receive terminals that diminish the line of sight between them. More precisely, thermal expansion, strong wind and weak earthquakes result in the sway of the high–rise buildings where the optical wireless terminals are usually located, and thus, optical beam vibrations are occurred which result, in turn, in significant misalignment-induced irradiance fluctuations at the receiver's side [12], [87]-[89]. The pointing errors create a random effect, and thus, in order to emulate its consequences, i.e., the misalignment-induced fading, we need an accurate distribution model. One such, widely utilized distribution model was first proposed by Farid *et al*. in [12], considering detector aperture size, beam width and jitter variance through Rayleigh distribution. Typical examples in which this pointing error model is involved to derive the joint turbulence-induced and misalignment-induced fading could be found in [12], [16], [82], [88], [89]. Nonetheless, according to this model, the boresight component of pointing is assumed to be zero and both horizontal and elevation displacement are assumed to follow an independent, identically distributed zero-mean Gaussian distribution.

Although typical terrestrial FSO systems are initially installed with near zero boresight error, the boresight is still considerable due to the thermal expansion of the buildings [90]. Thus, in practical point of view pointing errors consist of both, nonzero boresight and jitter components. It should be mentioned here that the boresight is the fixed displacement between beam center and detector's center, while the jitter is the random offset of the beam center at detector plane, which is mainly caused by building sway and building vibration. In view of the above, Gappmair *et al*. in [91] extended the analysis carried out in [12] in order to assume different jitters for the elevation and the horizontal displacement, considering that the radial displacement at the receiver follows a Hoyt distribution. In [90], Yang et al. based once again on [12], derived a more generalized statistical model to describe the pointing error effects with non-zero boresight displacement, considering that the radial displacement at the receiver follows a lognormal-Rician distribution this time.

Recently, Ansari *et al*. extracted in [92] unified expression for the moments of the average SNR of a FSO link operating over lognormal, Rician-lognormal and *M*-(alaga) turbulent channels along with nonzero and zero boresight pointing errors. Based on these expressions they also presented in [92] unified asymptotic formulas applicable in a wide SNR range for the ergodic capacity in terms of simple elementary functions for the respective turbulence models. Then, AlQuwaiee *et al*. presented in [93] a more generalized pointing error approach through the versatile statistical Beckman distribution model that includes many distributions as special cases such as Rayleigh, Hoyt and lognormal-Rician among others. Additionally, they derived a generic expression of the asymptotic capacity of FSO systems under the joint impact of generalized pointing errors and Gamma-Gamma or lognormal modelled turbulence. More recently, Boluda-Ruiz et al. derived an approximate expression for the combined pdf with atmospheric turbulence and non-zero boresight pointing errors in [94] by introducing an efficient and accurate approximation of the Beckmann distribution, which is used to model generalized pointing errors with quite high precision [94].

In view of the above and considering also the growing interest that non-zero boresight pointing errors hypothesis has raised in technical literature recently [84], [90]-[95], in this work we focus on the model proposed in [94] in order to study the impact of non-zero boresight misalignment fading on RoFSO performance, as it will be presented in more detail below.

C. *Methods for RoFSO Performance Improvements*

In order to improve the performance of an FSO system impaired by the combined turbulence-induced and misalignment-induced fading, particular attention is given to the modulation format to be employed. Modulation techniques can be generally classified into two categories. The first is single-carrier modulation, in which the data are carried on a single main carrier. This is the "conventional" modulation format that has been the workhorse in optical communications for more than three decades.

Single-carrier modulation has in fact experienced rapid advancement in recent years [96]. Indeed, the most widely utilized modulation format in the commercial and research field is the On-Off Keying (OOK) with Intensity Modulation/Direct Detection (IM/DD) signaling technique, mainly due to its simplicity [91]. However, it requires an adaptive threshold to optimally perform in turbulent atmosphere [39], [45]. This drawback may be circumvented via Pulse Position Modulation (PPM) technique, although it performs a spectral efficiency much lower than that of OOK signals [46], [91]. The second category of modulation technique is multicarrier transmission, in which the data are carried through many closely spaced subcarriers, [96]. Thus, an effective alternative to both OOK and PPM schemes is the Subcarrier Intensity Modulation (SIM) technique that was first suggested in [97] for optical wireless links. In a SIM FSO system a pre-modulated, usually with a Phase Shift Keying (PSK) modulation format and properly biased RF subcarrier is used to modulate the intensity of the optical carrier [98]. Therefore, by employing any multicarrier technique, like SIM, the performance of the optical wireless transmission is enhanced due to the fact that multiple subcarriers are used to carry the information and thus increased throughput is obtained.

Additionally, in the SIM FSO concept many works have been recently presented, [68], [71], [99]-[102]. Additionally, Orthogonal Frequency Division Multiple Access (OFDM) over optical link is a special class of multicarrier (multiple-subcarrier) intensity modulation category that has only recently gained significant attention in the optical communication community [9], [24], [25], [96], [98] and will be also employed in the current work below. In basic terms, OFDM refers to data transmissions in parallel on a number of different frequencies, while the subcarrier frequencies are chosen so that the signals are mathematically orthogonal over one OFDM symbol period. In general, OFDM is one of the most popular techniques for broadband wireless communications and it is known for its increased robustness against frequency selective fading, intersymbol and narrow-band interference, as well as for its high channel efficiency.

Consequently, it has been adopted in a wide range in the RF domain including digital audio/video broadcasting (DAB/DVB), wireless local area networks (LANs) also known as IEEE 802.11a/g or Wi-Fi, assymetric digital subcarrier line (ADSL; ITUG.992.1), wireless metropolitan area networks (WiMAX; 802.16e) and long-term evolution (LTE)-the fourth generation mobile communications technology [9], [96]. Nevertheless, the application of OFDM to optical domain occurred surprisingly late, mainly due to the fact that its robustness against optical channel dispersion was not recognized until Dixon et al. proposed in [103] the use of OFDM to combat modal dispersion in multimode fiber (MMF) channel that resembles that of the wireless one in terms of multipath fading [96]. However, Optical OFDM (O-OFDM) apart from interference immunity due to its orthogonality property and that multiple independent bit streams are modulated onto subcarriers at different frequencies multiplexed in the RF domain with IM/DD scheme offering high capacity links, it suffers mainly from the following drawbacks.

To begin with, the baseband OFDM signal is complex and bipolar, while IM/DD requires a real and positive RF signal to drive the laser diode (LD). Therefore, we need to transform the OFDM signal to unipolar by adding for instance a DC bias to the OFDM signal (DC-OFDM; DCO-OFDM) so that the resulting signal becomes positive [104]. Note that this DC bias should be large enough to prevent clipping and distortion in the optical domain [9], [73]. The latter translates into average optical power inefficiency especially for IM/DD DC-OFDM (DCO-OFDM), while the large number of subarriers creates unfavorable high peak-to-average power ratios (PARP) and finally distortions due to LD nonlinearties may be occurred [1], [73], [105]. Still, OFDM remains a very well-established modulation scheme for modern broadband communication systems such as OFDM-over-FSO or RoFSO as it is demonstrated both theoretically and experimentally in [9], [24], [25], [34], [73], [106]-[108]. Moreover, it should be mentioned that in order to successfully apply OFDM to FSO some additional OFDM modification techniques are proposed such as asymmetrically clipped O-OFDM (ACO-OFDM), flipped OFDM (Flip-OFDM), unipolar OFDM (U-OFDM) and instead of direct-detection O-OFDM (DDO-OFDM) the coherent O-OFDM (CO-OFDM), [96], [98], [109]-[112].

As already mentioned above, the negative consequences of atmospheric turbulence on FSO and RoFSO transmissions are getting worse as the optical signal is propagating over longer distances. Thus, especially for link ranges longer than 1km, the combined turbulence-induced and misalignment induced fading becomes a major performance and coverage area limiting factor in such wireless systems. A very promising technique to combat this distance-dependency of the combined turbulence-induced and misalignment-induced fading is the use of relays that create intermediate shorter hops and thus they can lead to longer (total) link length and performance improvements. Relay-assisted links may employ either DF or Amplify-and-Forward (AF) relays that may be connected either serially (i.e. multi-hop transmission) or in parallel (i.e. cooperative diversity).

In serial, i.e. multi-hop, DF relaying configurations the source transmits the information signal to the nearest DF relay node, which decodes the signal after detection, modulates it and retransmits it to the next relay or the destination only if the received SNR exceeds a specific decoding threshold that provides proper and reliable operation of the communication system. This process continues until the source’s data arrives at the destination node. Note that one such multi-hop DF configuration will be analyzed as part of the current work. Similarly, for multi-hop AF transmissions the same procedure applies with the sole difference that each relay does not perform any decoding on the received signal but after a multiplication with a proper energy scaling term (amplification), simply forwards it to next relay or the destination.

Additionally, in parallel relying configurations the source transmits the same signal to all relays, which, in turn, either decode and retransmit the signal (case of DF relays) or amplify and forward it (case of AF relays) to the destination [23], [113]-[117]. Over the last years the use of relay-assisted optical wireless transmissions has been discussed in many works in the open technical literature. Their results highlight the usefulness of relay-assisted transmission as a method to effectively broaden the optical wireless coverage area or as a fading-mitigation tool, [23], [83], [106], [113]-[121].

D. Motivation

By focusing on the issue of OFDM-based RoFSO transmissions and by considering the above phenomena and techniques, a lot of interesting work has been recently done. In [9], Bekkali et al. examined the performance of a RoFSO QAM or PSK OFDM IM/DD link over weak to strong turbulence conditions, modeled by Gamma-Gamma distribution. By using the closed-form expressions they derived they proved that RoFSO performance is highly sensitive to the atmospheric turbulence and the received optical power, while they also demonstrated that selecting an appropriate optimal optical modulation index (OMI) it is feasible to upgrade the overall RoFSO system performance. Later, Tsonev et al., first proposed in [109] an U-OFDM scheme for FSO that provides the same benefits of ACO-OFDM modulation, as well as improved demodulation for better power efficiency in Additive White Gaussian Noise (AWGN) channel, while when compared to DCO-OFDM, the proposed scheme showed better performance results in terms of BER. Next, the analysis performed Selvi and Murugesan in [34] showed that over weak turbulence conditions 3-5dB improvement is obtained for RoFSO QAM or PSK OFDM transmission compared to RF based wireless transmission. Then, Dimitrov *et al.*, studied in

[111] the double-sided signal clipping in ACO-OFDM FSO systems due to biasing issues and physical limitations of the transmitted front-end. They showed that unlike in OFDM-based RF systems, an SNR increase is not achievable simply by increasing the average electrical and/or optical power at the transmitter since the latter leads to a larger clipping distortion, and therefore, to a larger SNR penalty. Additionally, they found that ACO-OFDM is more robust to the clipping effects than DCO-OFDM for similar modulation schemes at the expense of a 50% reduction in spectral efficiency and thus, that ACO-OFDM is more suitable for applications with lower radiated average optical power, whereas DCO-OFDM promises to deliver higher throughput. Later, Tsonev et al., presented in [110] a complete analytical framework for the analysis of memoryless nonlinear distortion in an FSO system that guarantees closed-form solutions, assuming DCO-OFDM, ACO-OFDM, U-OFDM and pulse amplitude modulated discrete multitone modulation (PAM-DMT) along with QAM and PAM modulation formats.

In this context, Nistazakis et al. investigated in [73] the influence of non-lineal clipping effect along with Gamma-Gamma turbulent channel and they derived mathematical expressions for the estimation of the average SNR, average BER and the outage probability as a function of the physical parameters of the OFDM FSO link. Additionally, Nistazakis *et al*. in [23] extended the work in [9] by studying the performance of a DF multi-hop RoFSO QAM or PSK OFDM system over Gamma Gamma or negative exponential turbulent channels. They demonstrated that the use of relays increases the RFO coverage area but at the expense of increased BER values, while they extracted useful closed-form expressions for the BER estimation and the design of either single RoFSO QAM or PSK OFDM links or relayed systems, according to the specific turbulence conditions, modulation format and (each) link's individual parameters, based on the demands of OFDM RoFSO configuration. More recently, Nistazakis *et al*., in [122] extended even more the performance studies in [9] and [24], by investigating the performance of a DF multi-hop QAM RoFSO system under the presence of Gamma-Gamma or Gamma turbulence along with pointing errors.

Nevertheless, to the best of author's knowledge, there isn't any work that investigates the combined impact of both turbulence and non-zero boresight pointing error effects of a relay-assisted OFDM-based RoFSO system in the open literature so far. Thus, the performance of typical multi-hop DF relay-assisted QAM-OFDM RoFSO systems under the combined impact of a wide range of *M*-alaga turbulent conditions along with weak to strong non-zero boresight pointing errors is addressed in the current work. More specifically, we initially derive novel closed-form expressions for the average BER (ABER) and the outage probability (OP) of each intermediate RoFSO hop and by using them we next derive novel closed-form expressions for ABER and the OP of the total multi-hop system. In this context, we aim to reveal that the use of DF relays can significantly broaden the RoFSO coverage area but at the expense of increased ABER and OP values compared to the initial shorter link.

Moreover we intend to demonstrate the impact of average CNDR, the number of relays and the value of the modulation order L of the employed L-QAM format on the RoFSO performance. Additionally, we aim to prove that for specific link's characteristics the use of DF relays can be considered as a fading-mitigation tool that improves the RoFSO performance for the same total link length. Proper numerical results are provided, validated by simulations that demonstrate the accuracy of our derived expressions. Note that in order to further verify our suggestions, apart from the numerical and simulation results obtained for the RoFSO link we have assumed, we also obtained further numerical and simulation results for a practical link, by using some experimental measurements performed in University of Waseda, Japan, on the 15th October, 2009, as it was presented in [82].

II. System Model

A. Basic Principles of the Examined RoFSO System

The total RoFSO system under consideration consists of the initial transmitter, the final receiver and between them (H-1) serially connected DF relay nodes, which create H individual intermediate optical links. Note that in order to optimize the performance of the system the DF relay nodes are placed equidistant along the direct line from source to the destination, as it was shown in [114]. The laser diode (LD) at the initial transmitter's side emits an optical OFDM signal, modulated with L-QAM modulation scheme, towards the receiver of the nearest relay node where it may be decoded and retransmitted to the next DF relay. In fact, OFDM is an effective way of multicarrier transmission where the data is transmitted in parallel and thus simultaneously, by splitting into multiple narrow band subcarriers. Thus, each RF subcarrier (our case of RoFSO) is modulated with a L-QAM format and then carried on a high frequency optical carrier emitted by LD. Recall that the subcarriers of the OFDM are orthogonal to each other since their set is realized by using the inverse fast Fourier transform (IFFT) at the transmitter and the fast Fourier transform (FFT) at the receiver, and hence the inter-symbol interference (ISI) between them is minimal allowing easier signal detection at the receiver using standard correlation techniques [9], [23]. In order to study the total system's performance, we first focus on its fist intermediate link. The information signal is loaded in the N RF subcarriers and thus, the OFDM signal, $s_{OFDM}(t)$, after the up-conversion to the carrier frequency, f_c, just before the LD transmitter, is given as [9], [25]:

$$\begin{aligned} s_{OFDM}(t) &= \sum_{n=0}^{N-1} s_n(t) \qquad , \quad 0 \le t < T_s \qquad (1) \\ &= \sum_{n=0}^{N-1} X_n \exp\left[i\left(\omega_n + 2\pi f_c\right)t\right] \end{aligned}$$

where $\omega_n=2\pi/T_s$, $n=0,..N$-1, represents the angular frequency of each of the N orthogonal subcarriers, T_s is the duration of the OFDM symbols, while X_n stands for the complex data symbol of the n_{th} subcarrier, which is mapped according to selected modulation format, which here, is the L-QAM scheme with L being 4, 16 or 64, [9].

The above OFDM signal modulates the optical intensity of the LD at the transmitter's side and owing to the non-linearity of the latter device its emitted optical power, $P(t)$, is given as [1], [9], [23]:

$$P\left(t\right)=P_t\left[1+\sum_{n=0}^{N-1}m_n s_n\left(t\right)+a_3\left(\sum_{n=0}^{N-1}m_n s_n\left(t\right)\right)^3\right], \tag{2}$$

where P_t represents the average transmitted optical power, a_3 stands for the third order non-linearity coefficient of the LD and m_n is the optical modulation index (OMI) of the n_{th} subcarrier, [9]. Additionally, the optical power that arrives at the receiver of the nearest to the initial transmitter DF relay node, should be equal to [9], [23]:

$$P_r\left(t\right)=P\left(t\right)L_{tot}I+n(t), \tag{3}$$

where L_{tot} represents the overall attenuation losses caused by atmosphere, I stands for the instantaneous normalized received irradiance that arrives at the receiver of the DF relay node and $n(t)$ is the AWGN of the channel, [24]. Here, it should be mentioned that the instantaneous normalized received irradiance I is fluctuated randomly at the receiver's side due to both turbulence-induced and misalignment-induced fading. Thus it holds that $I=I_t I_p$, where I_t stands for the instantaneous normalized received irradiance due to atmospheric turbulence-induced fading and I_p represents the instantaneous normalized received irradiance due to misalignment-induced fading, respectively, [12], [16], [81]. Moreover, from Eqs (2) and (3), the output current at the receiver's photo-diode (DP) of the examined DF relay is expressed as [9], [23]:

$$i\left(t,I\right)=I_0\left[1+\sum_{n=0}^{N-1}m_n s_n\left(t\right)+a_3\left(\sum_{n=0}^{N-1}m_n s_n\left(t\right)\right)^3\right]+n_{opt}\left(t\right), \tag{4}$$

where $I_0=\eta L_{tot}P_t I$ is the direct current (DC) component of the received photo-current $i(t,I)$, η stands for the PD responsivity and $n_{opt}(t)$ represents the AWGN with zero mean and variance equal to the half of the noise power, i.e., $N_0/2$, obtained as $N_0=4K_B TF/R_L+2qI_0+I_0^2\left(RIN\right)$, where K_B, T ,F, R_L, q and RIN represent the Boltzmann's constant, the temperature, the noise figure of the receiver, the electron charge and the relative intensity noise *(RIN)* process, respectively, [9], [24]. Furthermore, another performance mitigation factor that cannot be neglected is the effect of inter-modulation distortion (IMD) due to the finite linear operating range of the LD transmitter. This IMD noise for the N subcarriers is expressed as [9], [23]:

$$\sigma_{IMD,n}^2=\frac{9a_3^2 m_n^6 I_0^2}{128}\times \times\left(2n\left(N-n+1\right)+N\left(N-5\right)+2-\frac{\left(-1\right)^n-\left(-1\right)^{2N+n}}{2}\right)^2. \tag{5}$$

Consequently, from (4) and considering also the presence of IMD noise in (5) and that the total noise (IMD and optical noise) are Gaussian distributed we obtain that the instantaneous carrier to noise plus distortion which is arriving at the receiver of the examined DF relay node, for each of the N subcarriers, n, is given by the following approximation [9], [10], [23], [106]:

$$CNDR_n\left(I\right)\approx\frac{m_n^2\eta^2 L_{tot}^2 P_t^2 I^2}{2\left(N_0/T_s+\sigma_{IMD,n}^2\right)}, \tag{6}$$

Similarly, the expected value of the $CNDR_n$, i.e., $CNDR_{n,EX}$, can be obtained from (6) as follows:

$$CNDR_{n,EX}\approx\frac{\left(m_n\eta L_{tot}P_t\, E\left[I\right]\right)^2}{2\left(\left[N_0/T_s\right]_{AV}+\left[\sigma_{IMD,n}^2\right]_{AV}\right)}. \tag{7}$$

where the symbol $[.]_{AV}$ stands for the average value.

We ought to declare here that considering the presence of (non-zero boresight) pointing error effects we cannot set $E[I]$=1 in (7) as is the case of [23, Eq. (10)] where negligible pointing error effects are considered.

B. Atmosheric Turbulence Over the RoFSO Channel

In order to accurately emulate the atmospheric turbulence-induced fading, i.e., the random and rapid scintillations of the received irradiance that significantly mitigate both the RoFSO performance and coverage area, as explained above, we are using the recently-launched and unifying *M-alaga*-distribution model which is very accurate for weak to strong turbulence conditions. According to this versatile model, the turbulence-induced fading I_t (i.e., the normalized irradiance at the receiver of the DF relay due to turbulence conditions prevailing along the individual hop) is considered as a random variable with the following PDF, [79], [82]:

$$f_{I_t}(I_t)=A_{(\aleph\text{ or }\Re)}\sum_{(\aleph\text{ or }\Re)}a_{k(\aleph\text{ or }\Re)}I_t^{\frac{a+k-2}{2}}K_{a-k}\left(2\sqrt{B_{(\aleph\text{ or }\Re)}I_t}\right), \tag{8}$$

where the subscripts $\aleph$ or $\Re$ correspond to the type of the parameter b i.e. being a natural or a real number, [24]. Thus, for $b\in\aleph$, the summation of the above PDF expression, Eq. (3), corresponds to $\sum_{(\aleph)}\left[.\right]=\sum_{k=1}^{b}\left[.\right]$ while, $A_{(\aleph)}=2a^{\frac{a}{2}}\left(bc\right)^{b+\frac{a}{2}}\Big/\left[c^{\frac{a+2}{2}}\Gamma\left(a\right)\left(bc+\Omega\right)^{b+\frac{a}{2}}\right]$, $B_{(\aleph)}=ab/(bc+\Omega)$ $a_{k(\aleph)}=\binom{b-1}{k-1}\left(\frac{\left(bc+\Omega\right)^{1-\frac{k}{2}}}{\left(k-1\right)!}\right)\left(\frac{\Omega}{c}\right)^{k-1}\left(\frac{a}{b}\right)^{\frac{k}{2}}$. On the other hand, for $b\in\Re$, $A_{(\Re)}=\left[2a^{a/2}(bc)^b\right]\Big/\left[c^{a+b/2}\Gamma(a)(bc+\Omega)^b\right]$,

$a_{k(\Re)}=(b)_{k-1}(ac)^{k/2}c^{1-k}(\Omega+cb)^{1-k}((k-1)!)^{-2}$ and $B_{(\Re)}=a/c$, where $(b)_k$ denotes the Pochhammer symbol, [79]. Moreover, $K_v(.)$ is the v_{th} order modified Bessel function of second kind, $\Gamma(.)$ is the Gamma function, a is a positive parameter related to the effective number of large scale cells of the scattering and $c=2b_0(1-\rho)$, [24]. The values of b_0 and ρ depend on the total scatter components and terms, while Ω is the average optical power of the coherent contributions which consists on the LOS and the coupled to the LOS scattering term, [24], [79], [82]. The parameter ρ indicates the relationship between the two scattering components of the *M-alaga* model mentioned above and represents the amount of scattering power coupled to the LOS component, while it ranges from zero to one, i.e., $0\le\rho\le 1$, [79], [82].

C. Nonzero Boresight Pointing Errors

The pointing errors effect consists of two components: the boresight and the jitter. The boresight is the fixed displacement between the beam center and the detector's center, while the jitter is the random offset of the beam center at the detector plane, [90], [95]. A general and realistic statistical distribution model which describes accurately the pointing errors effect taking into account the effect of beam width, the detector's size, the different jitters for the elevation, the horizontal displacement and the effect of non-zero boresight error is the Beckmann model which has the following PDF, [90], [94]:

$$f_R(R)=\frac{R}{2\pi\sigma_x\sigma_y}\times\int_0^{2\pi}\exp\left(-\frac{(R\cos\theta-\mu_x)^2}{2\sigma_x^2}-\frac{(R\sin\theta-\mu_y)^2}{2\sigma_y^2}\right)d\theta, \tag{9}$$

where θ is the transmit divergence angle describing the increase in beam radius with distance z from the transmitter. Note that the beam width can be approximated as $w_z\approx\theta z$ for relatively long distances. Additionally, R is the radial displacement that is expressed as $R=|\vec{R}|=\sqrt{R_x^2+R_y^2}$ where $\vec{R}=[R_x,R_y]^T$ is the radial displacement vector with R_x and R_y representing the displacements located along the horizontal and elevation axes at the detector plane, respectively. These random variables are considered as nonzero mean Gaussian distributed random variables, i.e., $R_x\sim N(\mu_x,\sigma_x^2)$, $R_y\sim N(\mu_y,\sigma_y^2)$ where the parameters μ_x, μ_y denote theirs mean values and σ_x, σ_y, the jitters for horizontal and elevation displacements respectively, [94]. The expression of Eq. (9) can be simplified, through the analysis performed in Ref. [94], and the Beckmann's distribution can accurately be approximated through the modified Rayleigh distribution, as follows, [94]:

$$f_R(R)=\frac{R}{\sigma_{\text{mod}}^2}\exp\left(-\frac{R^2}{2\sigma_{\text{mod}}^2}\right),\quad R\ge 0 \tag{10}$$

where $\sigma_{\text{mod}}^2=\left(\frac{3\mu_x^2\sigma_x^4+3\mu_y^2\sigma_y^4+\sigma_x^6+\sigma_y^6}{2}\right)^{1/3}$.

The PDF for the irradiance depending on the pointing errors effect, I_p, is approximated as, [94]:

$$f_{I_p}(I_p)=\frac{\psi^2}{(A_0 g)^{\psi^2}}I_p^{\psi^2-1},\ \text{for}\ 0\le I_p\le gA_0 \tag{11}$$

where $\psi=w_{z,eq}/2\sigma_{\text{mod}}$, $\psi_x=w_{zeq}/2\sigma_x$, $\psi_y=w_{zeq}/2\sigma_y$ and $g=\exp\left(\frac{1}{\psi^2}-\frac{1}{\psi_x^2}-\frac{1}{\psi_y^2}-\frac{\mu_x^2}{2\sigma_x^2\psi_x^2}-\frac{\mu_y^2}{2\sigma_y^2\psi_y^2}\right)$, [90], [94], [95].

We should recall here that any increase in the parameter ψ value translates into weaker amount of pointing mismatch, while w_{zeq} represents the equivalent beam radius at the receiver, which is given as $w_{zeq}=\left[\sqrt{\pi}\,\text{erf}(v)w_z^2/2v\exp(-v^2)\right]^{1/2}$ where $v=\sqrt{\pi}r_a/\sqrt{2}\,w_z$, r_a is the radius of the circular detection aperture and *erf*(.) stands for the error function. Notice that $A_0=[\text{erf}(v)]^2$, where A_0 is the fraction of the collected power at $r_a=0$, [12], [89], [94].

It is also notable that when the boresight displacement $s=\sqrt{\mu_x^2+\mu_y^2}$ is equal to zero, (i.e., $s=0$ and thus $\mu_x=\mu_y=0$) and $\sigma_x=\sigma_y$ the Beckmann's distribution of the non-zero boresight pointing errors above specializes to the Rayleigh's distribution of the zero boresight, in [12]. Thus, in this case equation (10) reduces to [1, Eq (10)] and equation (11) reduces to [1, Eq (11)].

D. Combined Impact of Turbulence and Pointing Errors

Once we obtained the PDFs of the turbulence-induced fading I_t and the misalignment induced fading I_t we can now estimate their combined impact through their joint PDF of the random variable $I=I_tI_p$. Thus, the combined PDF, $f_{comb,I}(I)$, for the normalized irradiance I, which arrives at the receiver's DF relay node side, is given through the following integral, [12], [16], [94]:

$$f_I(I)=\int f_{I|I_t}(I|I_t)f_{I_t}(I_t)dI_t, \tag{12}$$

where $f_{I|I_t}(I|I_t)$ stands for the conditional probability given I_t. Thus, by using (8) and by following the analysis performed in [12], [26], [94] we get:

$$f_I(I)=\frac{\psi^2 A_{(\aleph or \Re)}}{g^{\psi^2}A_0^{\psi^2}}I^{\psi^2-1}\times\sum_{(\aleph or \Re)}a_{k(\aleph or \Re)}\int_{I/A_0}^{\infty}I_t^{\frac{a+k-2\psi^2-2}{2}}K_{a-k}\left(2\sqrt{B_{(\aleph or \Re)}I_t}\right)dI_t. \tag{13}$$

The integral of (13) can be solved by representing the modified Bessel function in terms of Meijer's G-functions by using [123, Eq. (07.34.03.060.501)] and then, by using [123, Eq. (07.34.21.0085.01)]. Further, we apply [123, Eq. (07.34.17.0011.01)] and we conclude to the following closed-form expression for the combined turbulence-induced and non-zero boresight misalignment-induced fading.

$$f_I(I) = \frac{\psi^2 A_{(\aleph or \Re)} B_{(\aleph or \Re)}}{2A_0 g} \sum_{(\aleph or \Re)} a_{k(\aleph or \Re)} B_{(\aleph or \Re)}^{-\frac{a+k}{2}} \times G_{1,3}^{3,0}\left(\frac{B_{(\aleph or \Re)}}{A_0 g} I \middle| \begin{matrix} \psi^2 \\ \psi^2-1, \quad a-1, \quad k-1 \end{matrix} \right), \tag{14}$$

where $G_{p,q}^{m,n}[.]$ stands for the Meijer-function that is a standard built in function which can be evaluated with most of the well known mathematical software packages, [124].

Additionally, the expected value of the random variable I can be estimated by solving the following integral, [84]:

$$E[I] = \int_0^\infty I \; f_I(I) dI. \tag{15}$$

Thus, by substituting (14) into (15), and after some calculations, [81], the expected value of the random variable I is obtained as follows:

$$E[I] = A_0 g (c+\Omega) \big/ (\psi^{-2}+1). \tag{16}$$

III. AVERAGE BER OF THE L-QAM ROFSO SYSTEM

A. ABER for Each Individual OFDM RoFSO Link

One of the most well-known and crucial metric for the performance estimation of every communication system is the Bit Error Rate (BER), [18], [122], [125]. For our examined RoFSO system, we will first estimate the average BER (ABER) of each one of the h = 0, 1, 2,.., H, individual hops (for instance the ABER of the first hop, i.e., the nearest to the initial transmitter as mentioned above). Next, through the derived ABER expression of each individual link, the total ABER of the whole DF relayed multi-hop system will be estimated.

Assuming that Gray-coded mapping is used at the initial transmitter side and Gaussian distributed total noise in (6) as re-assumed above, the accurate ABER expression of an N-subcarriers L-QAM OFDM individual RoFSO link can be derived by averaging over all the N OFDM subcarriers, i.e., [9], [24], [125]:

$$P_{b,av}^{L-QAM} = \frac{4(1-L^{-1/2})}{N \log_2(L)} \times \sum_{n=0}^{N-1} \int_0^\infty \left\{ Q\left(\sqrt{\frac{3CNDR_n(I)}{L-1}} \right) - (1-L^{-1/2}) Q^2\left(\sqrt{\frac{3CNDR_n(I)}{L-1}} \right) \right\} f_I(I) dI, \tag{17}$$

where $Q(.)$ stands for the well-known Q-function and as mentioned above L corresponds to the modulation index of the QAM format [125].

In order to solve the integral of Eq. (17) we are using the recently presented following approximation, $Q^2(x) \approx \left[\exp(-x^2/2) + 4\exp(-11x^2/20) + 5\exp(-2x^2)\right]^2 \big/ 576$, [126]. After these substitutions, we represent both the exponential and the complementary error function quantities in terms of Meijer-G functions by using [123, Eq. (07.34.03.0228.01)] and [123, Eq. (07.34.03.0282.01)]. Thus, by substituting also (14) into (17), we obtain integrals that entail products of two Meijer-G functions as factors. This kind of integrals can be solved by using [123, Eq. (07.34.21.0013.01)]. Next, by performing all these cumbersome calculations and by using when feasible [123, Eq. (07.34.03.0001.01)] for simplification reasons, we conclude to the following closed form mathematical expression for the ABER of each L-QAM OFDM RoFSO individual link of our examined system under M-turbulent and non-zero boresight misalignment fading conditions:

$$P_{b,av}^{L-QAM} = \frac{4(1-L^{-1/2})}{576 N \log_2(L)} \times \sum_{n=0}^{N-1} \sum_{(\aleph or \Re)} \left[\frac{144}{\sqrt{\pi}} \frac{\xi}{(1-L^{-1/2})} \varphi - \xi\zeta\left(\frac{1008}{20}\right) - \xi\zeta(120) - \xi\zeta\left(\frac{2448}{20}\right) - \frac{1}{2}\xi\zeta(48) - \frac{1}{2}\xi\zeta\left(\frac{1056}{20}\right) - \frac{1}{2}\xi\zeta(192) \right], \tag{18}$$

where $\varphi = G_{6,3}^{2,5}\left(\frac{24A_0^2 g^2 \gamma}{(L-1)B_{(\aleph or \Re)}^2} \middle| \begin{matrix} \frac{2-\psi^2}{2}, & \frac{1-a}{2}, & \frac{2-a}{2}, & \frac{1-k}{2}, & \frac{2-k}{2}, & 1 \\ 0, & \frac{1}{2}, & \frac{-\psi^2}{2} & & & \end{matrix} \right)$,

$$\zeta(x) = G_{5,2}^{1,5}\left(x\beta \middle| \begin{matrix} \frac{2-\psi^2}{2}, & \frac{1-a}{2}, & \frac{2-a}{2}, & \frac{1-k}{2}, & \frac{2-k}{2} \\ 0, & \frac{-\psi^2}{2} & & & \end{matrix} \right),$$

$$\xi = \frac{\psi^2 A_{(\aleph or \Re)} 2^{a+k-2} a_{k(\aleph or \Re)} B_{(\aleph or \Re)}^{-\frac{a+k}{2}} (1-L^{-1/2})}{2\pi}, \quad \beta = \frac{A_0^2 g^2 \gamma}{B_{(\aleph or \Re)}^2 (L-1)}$$

and thus, $\gamma = \frac{m_n^2 \eta^2 L_{tot}^2 P_t^2}{2\left([N_0/T_S]_{AV} + [\sigma_{IMD,n}^2]_{AV}\right)}$, which from Eqs (7) and (16) it ends up to the mathematical expression, $\gamma = \frac{CNDR_{n,EX}}{(E[I])^2} = \frac{(1+\psi^{-2})^2}{A_0^2 g^2 (c+\Omega)^2} CNDR_{n,EX}$. In this context, we correspondingly obtain the following equivalent expressions

$$\varphi = G_{6,3}^{2,5}\left(\frac{24(1+\psi^{-2})^{-2} CNDR_{n,EX}}{(L-1)(c+\Omega)^2 B_{(\aleph or \Re)}^2} \middle| \begin{matrix} \frac{2-\psi^2}{2}, & \frac{1-a}{2}, & \frac{2-a}{2}, & \frac{1-k}{2}, & \frac{2-k}{2}, & 1 \\ 0, & \frac{1}{2}, & \frac{-\psi^2}{2} & & & \end{matrix} \right),$$

$$\beta = \frac{(1+\psi^{-2})^{-2} CNDR_{n,EX}}{(L-1)(c+\Omega)^2 B_{(\aleph or \Re)}^2},$$

$$\zeta(x) = G_{5,2}^{1,5}\left(\frac{(1+\psi^{-2})^{-2} CNDR_{n,EX}}{(L-1)(c+\Omega)^2 B_{(\aleph or \Re)}^2} x \middle| \begin{matrix} \frac{2-\psi^2}{2}, & \frac{1-a}{2}, & \frac{2-a}{2}, & \frac{1-k}{2}, & \frac{2-k}{2} \\ 0, & \frac{-\psi^2}{2} & & & \end{matrix} \right).$$

B. Total ABER for the Multi-hop L-QAM OFDM RoFSO System

The total average BER of the RoFSO system under consideration with the H individual hops, connected with the (H-1) DF relay nodes that are connected both serially and equidistantly is expressed as [23], [106]

$$P_{b,av,TOTAL}^{L-QAM}=\sum_{i=1}^{H}\left[P_{b,av,i}^{L-QAM}\prod_{j=i+1}^{H}\left(1-2P_{b,av,j}^{L-QAM}\right)\right], \quad (19)$$

which is a closed-form expression by substituting (18) into (19).

IV. Outage Propability Estimation

A. Outage Probability for Each Individual Link

Another very significant metric for the availability and performance of any RoFSO communication system is the outage probability (OP), [18], [21], [24], [52], [120]. This metric shows the probability of the *CNDR* at the receiver falls below a specific threshold value $CNDR_{th}$, which represents the lower limit for receiver's acceptable operation [9], [18], [52]. Consequently, the outage probability for each individual RoFSO hop should be

$$\begin{aligned}P_{out}&=\frac{1}{N}\sum_{n=0}^{N-1}P_{out,n}=\\&=\frac{1}{N}\sum_{n=0}^{N-1}\Pr\left(I_n<I_{n,th}\right)=\frac{1}{N}\sum_{n=0}^{N-1}F_{I_n}\left(I_{n,th}\right),\end{aligned} \quad (20)$$

where $F_I(.)$ stands for the CDF .

Therefore, in order to estimate the outage probability of each individual link of the investigated OFDM RoFSO multi-hop system, we need to obtain the CDF of the random variable I by averaging its PDF given by (14). Hence,

$$\begin{aligned}F_{I_n}\left(I_{n,th}\right)&=\int_0^{I_{n,th}}f_{I_n}\left(I_{n,th}\right)dI_n\\&=\frac{\psi^2A_{(\aleph or \Re)}B_{(\aleph or \Re)}}{2A_0g}\sum_{(\aleph or \Re)}a_{k(\aleph or \Re)}B_{(\aleph or \Re)}^{-\frac{a+k}{2}}\\&\times\int_0^{I_{n,th}}G_{1,3}^{3,0}\left(\frac{B_{(\aleph or \Re)}}{A_0g}I_{n,th}\left|\begin{matrix}\psi^2\\\psi^2-1,\ a-1,\ k-1\end{matrix}\right.\right)dI_n.\end{aligned} \quad (21)$$

The integral of Eq. (21) is solved by using [123, Eq. (07.34.21.0084.01)], and thus, the expression (21) is written as:

$$\begin{aligned}F_{I_n}\left(I_{n,th}\right)&=\frac{\psi^2A_{(\aleph or \Re)}}{2}\sum_{(\aleph or \Re)}a_{k(\aleph or \Re)}B_{(\aleph or \Re)}^{-\frac{a+k}{2}}\\&\times G_{2,4}^{3,1}\left(\frac{B_{(\aleph or \Re)}}{A_0g}I_{n,th}\left|\begin{matrix}1,\ \psi^2+1\\\psi^2,\ a,\ k,\ 0\end{matrix}\right.\right).\end{aligned} \quad (22)$$

Taking into account the Eqs (6), (7) and (16), for $I=I_n=I_{n,th}$, and thus, we get:

$$I_{n,th}=\frac{A_0g\left(c+\Omega\right)}{1+\psi^{-2}}\sqrt{\frac{CNDR_n\left(I_{n,th}\right)}{CNDR_{n,EX}}}. \quad (23)$$

Hence, from (20), (22) and (23) the OP of each L-QAM OFDM RoFSO individual link impaired by both *M-alaga* turbulence-induced and non-zero boresight misalignment-induced fading, can be expressed by the following closed-form expression:

$$\begin{aligned}P_{out}&=\frac{\psi^2A_{(\aleph or \Re)}}{2N}\sum_{n=0}^{N-1}\sum_{(\aleph or \Re)}a_{k(\aleph or \Re)}B_{(\aleph or \Re)}^{-\frac{a+k}{2}}\times\\&\times G_{2,4}^{3,1}\left(\frac{B_{(\aleph or \Re)}\left(c+\Omega\right)}{1+\psi^{-2}}\sqrt{\frac{CNDR_n\left(I_{n,th}\right)}{CNDR_{n,EX}}}\left|\begin{matrix}1,\ \psi^2+1\\\psi^2,\ a,\ k,\ 0\end{matrix}\right.\right).\end{aligned} \quad (24)$$

B. Total Outage Probability for the Muliti-hop System

In serial DF relaying, an outage occurs when any of the intermediate individual links fails [114], [119], [121], [122], i.e., falls below the critical specific threshold which determines its proper operation.

The probability of at least one of the H individual links interrupts the whole examined system, is expressed as:

$$P_{out,TOTAL}=1-\prod_{h=1}^{H}\left(1-P_{out}\right). \quad (25)$$

Hence, by substituting Eq. (24) into (25) we obtain the following closed-form expression of the outage probability of the total DF relayed multi-hop L-QAM OFDM RoFSO examined system:

$$\begin{aligned}P_{out,TOTAL}&=1-\prod_{h=1}^{H}\left\{1-\frac{\psi^2A_{(\aleph or \Re)}}{2N}\sum_{n=0}^{N-1}\sum_{(\aleph or \Re)}a_{k(\aleph or \Re)}B_{(\aleph or \Re)}^{-\frac{a+k}{2}}\right.\\&\left.\times G_{2,4}^{3,1}\left(\frac{B_{(\aleph or \Re)}\left(c+\Omega\right)}{1+\psi^{-2}}\sqrt{\frac{CNDR_n\left(I_{n,th}\right)}{CNDR_{n,EX}}}\left|\begin{matrix}1,\ \psi^2+1\\\psi^2,\ a,\ k,\ 0\end{matrix}\right.\right)\right\}.\end{aligned} \quad (26)$$

V. Numerical Results

A. RoFSO System under Assumption

In this section by using the closed-form expressions derived above, (18), (19), (26), we present performance results by means of both quantities, i.e. average BER and outage probability. The RoFSO system under consideration may operate either with or without DF relays in multi-hop L-QAM OFDM configurations. The number of OFDM subcarries is fixed at N=1000, while three values for the QAM signal constellation L are assumed, i.e. L=4, 16 or 64. The operational wavelength of the system is fixed at λ=1.55 μm, while its receiver's aperture diameter, D, is set at 0.1 m. Furthermore, each of the h=1, 2...H hops are assumed to have the same, equal to 1 km, link length. When H=1 the system is not a relay-assisted one but a regular line of sight link. In the examined RoFSO links below, the number of relays (H-1), is varying from 0 to 10. In all investigated cases, the operation of this RoFSO system is assumed to be impaired by the combined influence of turbulence-induced and non-zero boresight misalignment-induced fading. In this context, a wide range of weak to strong turbulence conditions is assumed, modeled through the accurate *M-alaga* distribution model. More precisely, we examine the following M-parameter values, a=3, b=3, ρ=0.95 for strong and a=8, b=4, ρ=0.95 for weak turbulence conditions. In addition, in all cases we will present below, the average optical power of each RoFSO link is normalized, i.e., $\Omega+2b_0=1, \Omega=0.5, b_0=0.25$. Note that this simplification for the average optical power holds true, without loss of generality. As regards the pointing mismatch, we assume normalized beam width value w_z/r=10, as well as the normalized boresight error values are fixed at $\left(\mu_x/r,\mu_y/r\right)=\left(1,2\right)$, while different normalized jitter values, $\left(\sigma_x/r,\sigma_y/r\right)=\left(1.2,0.9\right)$, $\left(\sigma_x/r,\sigma_y/r\right)=\left(2.6,1.4\right)$ and $\left(\sigma_x/r,\sigma_y/r\right)=\left(3.6,2.7\right)$ are investigated that correspond to $\psi=3.5$, $\psi=2.0$ and $\psi=1.5$, respectively, i.e., to weak, moderate and strong amount of non-zero boresight pointing mismatch respectively. Moreover, the corresponding Monte Carlo simulations are presented by solid dots, which validate the results obtained. Note that in order to avoid excessively long simulation runtimes, we do not generate results for values lower than 10^{-6}.

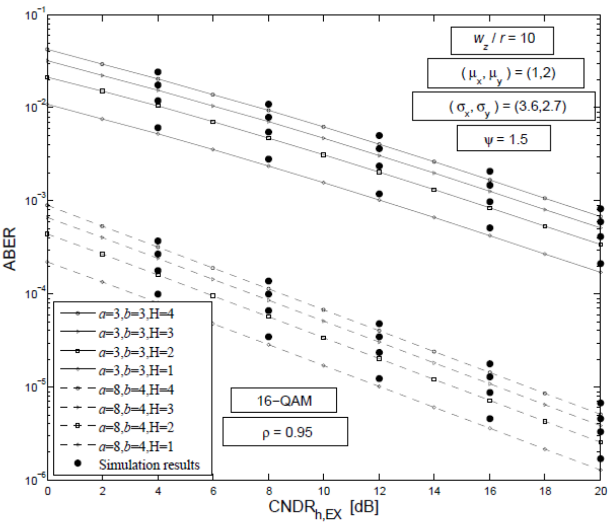

Fig. 1. Average BER of 16-QAM OFDM signals versus a wide range of CNDR for various number of RoFSO hops over weak to strong turbulence $\mathcal{M}$(alaga)-channels along with strong non-zero boresight misalignment-induced fading.

Fig. 1 illustrates the evolution of the ABER expressions (18) and (19) as a function of a wide range of expected *CNDR* at the receiver's side, of different number 16-QAM OFDM RoFSO links, under different *M*-turbulence conditions along with the same strong non-zero boresight misalignment-induced fading. Thus, the detrimental impact of atmospheric turbulence effect is highlighted in this figure. Indeed, as the atmospheric turbulence is getting weaker, i.e. as the parameters *a* and *b* obtain larger values -cases of *a*=8, *b*=4 that are visualized in dashed line style- it is clearly shown that decreased ABER values are obtained and thus, significant RoFSO performance improvements are depicted in this weak turbulence regime in comparison with the strong turbulence one i.e. cases of *a*=3, *b*=3. In each turbulence regime, four different hop-configurations are illustrated. As we can see, the increase of the number of hops *H* leads to longer RoFSO total link lengths. More specifically, each additional hop increases the total link length by 1 km but at the expense of increased ABER values, which translates into performance degradations in comparison with the initial shorter link. However, especially for high *CNDR* values, which significantly mitigate the ABER, the performance degradations due to DF relays employment are not proved to be so destructive to make the RoFSO system unreliable. In short, Fig. 1 reveals that the performance of a typical 16-QAM OFDM RoFSO DF relayed multi-hop system is significantly degraded by atmospheric turbulence, by decreased expected *CNDR* values and by employing a large number of DF relays connected in series, despite the far broadened coverage area they provide.

Fig. 2 depicts the evolution of the ABER expressions (18) and (19) as a function of the same wide range of expected CNDR at the receiver's side. The assumptions for the RoFSO system's characteristics are the same as in Fig. 1, but the parameter ψ in now fixed at a larger value that corresponds to a weaker amount non-zero boresight misalignment-induced fading. As we can observe, all the corresponding to Fig. 1 ABER values are significantly reduced. As a result, Fig. 2 compared to Fig. 1, demonstrates the performance-destructive impact of non-zero boresight pointing errors on RoFSO systems.

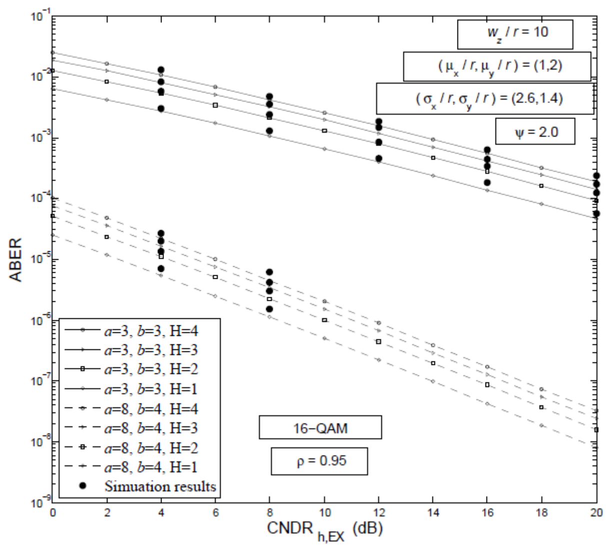

Fig. 2. Average BER of 16-QAM OFDM signals versus a wide range of CNDR for various number of RoFSO hops over weak to strong turbulence $\mathcal{M}$(alaga)-channels along with moderate non-zero boresight misalignment-induced fading.

Fig. 3 visualize the evolution of the ABER expressions (18) and (19) as a function of a wide range of the expected *CNDR* at the receiver's under strong *M*-alaga turbulence and moderate non-zero borsight pointing errors for different *L*-QAM formats, i.e. *L*=4, 16 or 64. The *L*-QAM OFDM RFSO system is considered to be a multi-hop one that may employ either 4 or 10 serially connected DF relays, which create *H*=5 or *H*=10 intermediate individual links, respectively. As it should be expected from the above, we unsurprisingly observe that the H=5 configuration, which is illustrated by dashed lines, outperforms in terms of ABER to the H=10 one. However, the latter configuration has the advantage of broader coverage area. Additionally in both multi-hop configurations it becomes evident that the lower order QAM schemes lead to significant performance enhancement. Thus, 4-QAM offers better ABER performance results than 16-QAM scheme, which outperforms, in turn, to 64-QAM format.

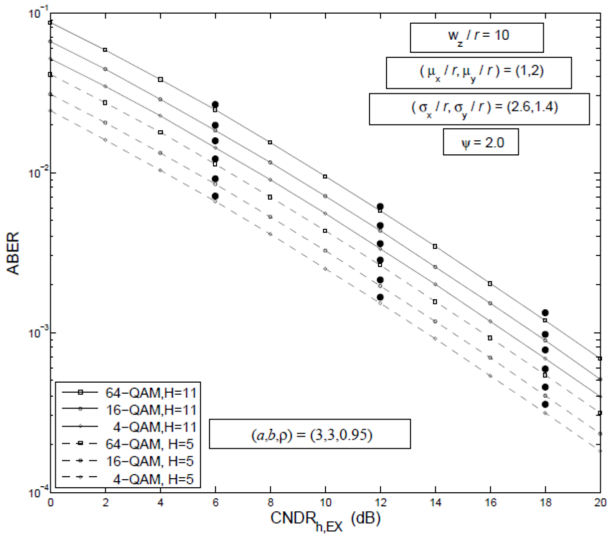

Fig. 3. Average BER of 4, 16, 64-QAM OFDM signals versus a wide range of CNDR for various number of RoFSO hops over strong turbulence $\mathcal{M}$(alaga)-channel along with moderate non-zero boresight misalignment-induced fading.

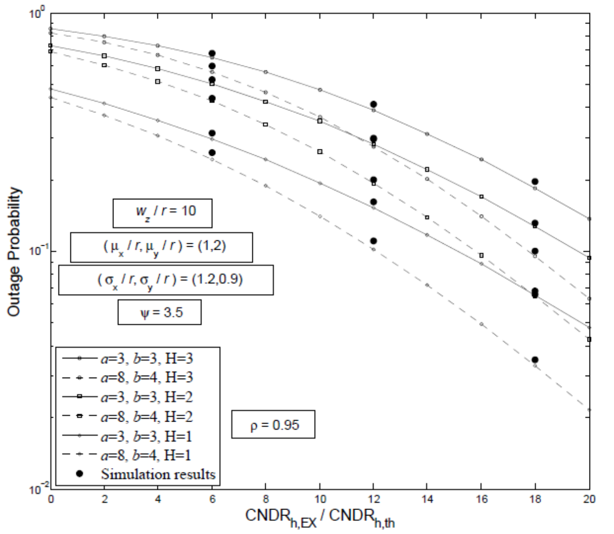

Fig. 4. Outage Probability estimation of single and multi-hop OFDM RoFSO systems over weak to strong turbulence $\mathcal{M}$(alaga)-channels along with weak non-zero boresight misalignment-induced fading.

Fig. 4 shows the OP results obtained by using (26) for a single-hop, a dual-hop and a triple-hop RoFSO OFDM system. This performance-metric is presented as a function of the normalized expected carrier to noise plus distortion, $CNDR_{h,EX}/CNDR_{h,th}$, at each DF receiver. Similarly to the ABER metric, the OP is showed to increase its value as the number of individual hops, or equivalently, as the number of DF relays employed increases. Once again, the increase of turbulence strength leads to further performance degradation, i.e. to further increase of the OP value. Consequently, especially under weak turbulence conditions, the single-hop system outperforms in terms of OP, while the triple-hop system outperforms in terms of coverage area.

Fig. 5 illustrates the OP results obtained by using (26) for the same RoFSO OFDM systems with Fig. 4, operating under the same turbulence conditions again, but under the presence of strong non-zero boresight pointing errors this time, as indicates the decrease of ψ parameter from 3.5 in Fig. 4, to 1.5 in Fig. 5. The comparison between these two figures reveals the detrimental impact of non-zero boresight pointing errors in terms of RoFSO outage probability.

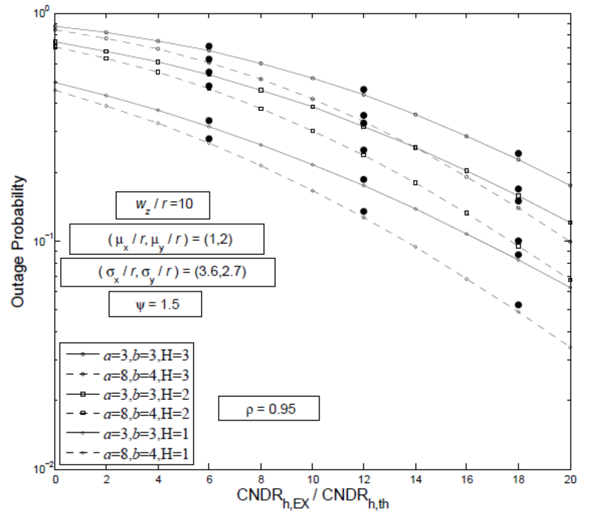

Fig. 5. Outage Probability estimation of single and multi-hop OFDM RoFSO systems over weak to strong turbulence $\mathcal{M}$(alaga)-channels along with strong non-zero boresight misalignment-induced fading.

B. Practical RoFSO System

In order to verify our proposed performance analysis on a practical level, we present here some numerical results derived by (26), but by adopting some experimental data measurements of a real optical wireless link, performed in University of Waseda, Japan, on the 15th October, 2009, as it was presented in [82]. This practical link operates with optical wavelength $\lambda = 785\,\mathrm{nm}$ and receiver's aperture diameter of 0.1m. Its length, i.e. the wireless FSO propagation distance from source to destination is $d_{SD} = 1\,\mathrm{km}$. Additionally, it is established at a height of 25 m above the sea level, while the optical power transmitted is 11.5 dBm with a responsivity of 0.8 A/W, [82].

We ought to recall here that the atmospheric turbulence is dependent on the Rytov variance, defined as $\sigma_R^2 = 1.23 C_n^2 \left(2\pi/\lambda\right)^{7/6} d_{SD}^{11/6}$, which is constant and takes a value $\sigma_R^2 = 0.36$ for the refractive index structure parameter $C_n^2 = 8.3 \times 10^{-15}\ \mathrm{m}^{-2/3}$ (which was measured on the 15th October 2009, at time 23:10), FSO propagation distance $d_{SD} = 1\,\mathrm{km}$ and employed $\lambda = 785\,\mathrm{nm}$. Considering that *M-alaga* distribution is a very accurate unifying model, the latter experimental-measured turbulence state for this specific practical link entirely corresponds to $(a,b,\rho) = (10,5,1)$ *M*-parameter values, as it is reported in Ref. [82]. Thus, this *M*-turbulent state $(a,b,\rho) = (10,5,1)$ will be used in our numerical results below. Similarly, another stronger *M*-turbulent state that results from experimental data and could be used below, is the state with $(a,b,\rho) = (10,5,0.25)$ that fully corresponds to a value $\sigma_R^2 = 1.2$ and $C_n^2 = 2.8 \times 10^{-14}\ \mathrm{m}^{-2/3}$ (which was measured on the 15th October 2009, near midday, [82]). Moreover, the non-zero boresight misalignment fading is fixed to be moderate and equal to all the examined cases. As a final remark, all cases that will be shown below were obtained, once again and without loss on generality, by employing the same normalized average optical power, i.e. $\Omega + 2b_0 = 1$, where $\Omega = 0.5$ and $b_0 = 0.25$.

In view of the above, Fig. 6 depicts three different OFDM RoFSO realizations of the investigated practical link. The most performance-effective in terms of outage probability is the original link's configuration over weak measured turbulence conditions, i.e. with $(a,b,\rho) = (10,5,1)$ and total link length equal to 1 km, without any DF relay employment. The same single-hop link, but under stronger turbulence conditions, i.e., $(a,b,\rho) = (10,5,0.25)$ and longer link length equal to 2 km is shown to obtain increased corresponding OP values compared to the immediately above case. This is due to the fact that stronger turbulent channels lead to more significant availability and performance RoFSO degradations, as well as, the increase of the propagation distance (without using relays) brings about stronger turbulence induced-fading at the receiver side. Finally, the third configuration, represented by a dashed line, is assumed to have also an extended total length of 2 km, but employs a DF relay which is assumed to be placed in the middle of the total link (i.e., dual-hop configuration with hop lengths equal to 1 km). The use of DF relay enables the dual-hop system to deal with a weaker amount of turbulence-induced fading in each hop than the second mentioned configuration, which despite having the same total link length of 2km it has to deal with a stronger amount of turbulence-induced fading at the receiver's side. This explains the better performance results that may offer the dual-hop scheme, compared to the second-mentioned configuration, provided that the receiver of the DF relay has the proper *CNDR* sensitivity limit. Consequently, apart from increasing the coverage RoFSO area, DF relays, may also be used as a fading-mitigation tool to combat the combined impact of turbulence and pointing errors.

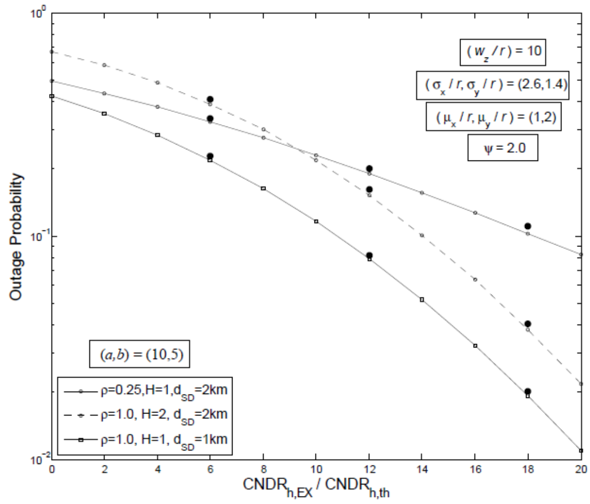

Fig. 6. Outage Probability estimation of three different configurations of a practical OFDM RoFSO system over weak to strong turbulence $\mathcal{M}$(alaga)-channels along with moderate non-zero boresight misalignment-induced fading.

VI. Conclusions

In this work, the combined impact of both *M*-alaga modeled turbulence and non-zero boresight pointing errors effect on the performance of a multi-hop DF relayed with *N*-subcarriers *L*-QAM OFDM RoFSO system is investigated. Thus, accurate enough closed-form expressions are derived for the fundamental ABER and the outage probability performance metrics of such RoFSO configurations. It was demonstrated that DF relays connected in series can significantly broaden the RoFSO coverage area, but at the expense of increased ABER and OP values, in comparison with the corresponding ABER and OP values of the initial shorter RoFSO link. Additionally, it was shown that by inserting serially connected DF relays in a RoFSO link we may improve its initial performance, since the resulting intermediate individual hops are shorter, and thus, they have to deal with a weaker amount of combined turbulence-induced and non-zero boresight misalignment-induced fading.

References

[1] H. Al-Raweshidy and S. Komaki, *Radio Over Fiber Technologies for Mobile Communications Networks*, 1st ed. Norwell, MA: Artech House, 2002, ch. 2, pp. 65-102.

[2] A. J. Cooper, "Fiber/Radio for the provision of cordless/mobile telephony services in the access network," *Electronics Letters*, vol. 26, no. 24, pp. 2054-2056, Nov. 1990.

[3] C. Cordeiro, H. Gossain, R. Ashok, and D. P. Agrawal, "The last mile: Wireless technologies for broadband and home networks," in *Proc. 21st Brazilian Symposium on Computer Networks*, May 2003, pp. 19-23.

[4] W. S. Chang, ed., *RF Photonic Technology in Optical Fiber Links*, Cambridge University Press, 1st ed., Oct. 2002, ch. 2, pp. 35-53.
[5] C. H. Cox, *Analog Optical Links: Theory and Practice*, Cambridge University Press, 1st ed., 2004, ch. 2, pp. 19-49.
[6] S. Hunziker and W. Baechtold, "Cellular remote antenna feeding: optical fibre or coaxial cable?" *Electronics Letters*, vol. 34, no. 11, pp. 1038-1040, 1998.
[7] K. Kazaura, K. Wakamori, M. Matsumoto, T. Higashino, K. Tsukamoto, and S. Komaki, "RoFSO: A universal platform for convergence of fiber and free-space optical communication networks," *IEEE Communications Magazine*, vol. 48, no. 2, pp. 130-134, Feb. 2010.
[8] Z. Ghassemlooy and W. O. Popoola, "Terrestrial free-space optical communications," in *Mobile and Wireless Communications: Network Layer and Circuit Level Design*, S. Ait Fares and F. Adachi, Eds., 2010.
[9] A. Bekkali, C. B. Naila, K. Kazaura, K. Wakamori, and M. Matsumoto, "Transmission analysis of OFDM-based wireless services over turbulent radio-on-FSO links modeled by gamma–gamma distribution," *IEEE Photonics Journal*, vol. 2, no. 3, pp. 510-520, June 2010.
[10] K. Prabu, S. Bose, and D. S. Kumar, "Analysis of optical modulators for radio over free space optical communication systems and radio over fiber systems," in *Proc. India Conference (INDICON), 2012 Annual IEEE*, December 2012, pp. 1176-1179.
[11] H. Hogan, "Data demands: Drive free-space optics," *Photonics Spectra*, vol. 47, no. 2, pp. 38-41, Feb. 2013.
[12] A. A. Farid and S. Hranilovic, "Outage capacity optimization for free-space optical links with pointing errors," *Journal of Lightwave Technology*, vol. 25, no. 7, pp. 1702-1710, 2007.
[13] R. Rachmani and S. Arnon, "Wavelength diversity in turbulence channels for sensor networks," in *Proc. IEEE 26th Convention of Electrical and Electronics Engineers in Israel*, 2010.
[14] H. Henniger and O. Wilfert, "An introduction to free-space optical communications," *Radioengineering*, vol. 19, no. 2, pp. 203-212, 2010.
[15] A. K. Majumdar, "Advanced Free Space Optics (FSO): A system approach," in *Springer Series in Optical Sciences, Springer Science and Business Media*, New York, 2015.
[16] G. K. Varotsos, H. E. Nistazakis, C. K. Volos, and G. S. Tombras, "FSO links with diversity pointing errors and temporal broadening of the pulses over weak to strong atmospheric turbulence channels," *Optik-International Journal for Light and Electron Optics*, vol. 127, no. 6, pp. 3402-3409, 2016.
[17] M. S. Awan, L. C. Horwath, S. S. Muhammad, E. Leitgeb, F. Nadeem, and M. S. Khan, "Characterization of fog and snow attenuations for free-space optical propagation," *Journal of communications*, vol. 4, no. 8, pp. 533-545, 2009.
[18] H. E. Nistazakis and G. S. Tombras, "On the use of wavelength and time diversity in optical wireless communication systems over gamma–gamma turbulence channels," *Optics & Laser Technology*, vol. 44, pp. 2088–2094, 2012.
[19] G. Ntogari, T. Kamalakis, and T. Sphicopoulos, "Performance analysis of space time block coding techniques for indoor optical wireless systems," *IEEE Journal on Selected Areas in Communications*, vol. 27, no. 9, 2009.
[20] W. O. Popoola, Z. Ghassemlooy, and E. Leitgeb, "BER and outage probability of DPSK subcarrier intensity modulated free space optics in fully developed speckle," *J. of Comm.*, vol. 4, no. 8, pp. 546-554, 2009.
[21] K. Prabu, S. Bose, and D. S. Kumar, "BPSK based subcarrier intensity modulated free space optical system in combined strong atmospheric turbulence," *Optics Communications*, vol. 305, pp. 185-189, 2013.
[22] V. W. S. Chan, "Free-space optical communications," *J. Lightwave Technol.*, vol. 24, no. 12, 2006, pp. 4750–4762.
[23] H. E. Nistazakis, A. N. Stassinakis, S. S. Muhammad, and G. S. Tombras, "BER estimation for multi hop RoFSO QAM or PSK OFDM communication systems over Gamma–Gamma or exponentially modeled turbulence channels," *Elsevier Opt. Laser Technol.*, vol. 64, pp. 106–112, Dec. 2014.
[24] H. E. Nistazakis, A. N. Stassinakis, H. G. Sandalidis, and G. S. Tombras, "QAM and PSK OFDM RoFSO Over M-Turbulence induced fading channels," *IEEE Photonics Journal*, vol. 7, no. 1, 2015.
[25] A. Mostafa and S. Hranilovic, "In-Field demonstration of OFDM-Over-FSO," *IEEE Photonics Technology Letters*, vol. 24, no. 8, pp. 709-711, 2012.
[26] K. Kazaura, K. Omae, T. Suzuki, *et al*., "Performance evaluation of next generation FreeSpace optical communication system," *IEICE Transactions on Electronics*, vol. E90-C, no. 2, pp. 381-388, 2007.
[27] P. T. Dat, A. M. Shah, K. Kazaura, K. Wakamori, T. Suzuki, *et al*., "Investigation of suitability of RF signal transmission over FSO links," in *Proc. International Symposium on High Capacity Optical Networks and Enabling Technologies*, 2007, pp. 1-6.
[28] N. Cvijetic and S. G. Wilson, "WiMAX access using optical wireless technology with heterodyne detection in turbulent atmospheric channels," in *Proc. IEEE GLOBECOM*, 2006, pp. 1-6.
[29] N. Cvijetic and T. Wang, "A MIMO architecture for IEEE 802.16d (WiMAX) heterogeneous wireless access using optical wireless technology," in *Next Generation Teletraffic and Wired/Wireless Advanced Networking*, Springer Verlag, 2006, pp. 441–451.
[30] S. Arnon, "Minimization of outage probability of WiMAX link supported by laser link between a high-altitude platform and a satellite," *J. Opt. Soc. Am. A*, vol. 26, no. 7, pp. 1545–1552, July 2009.
[31] N. Vaiopoulos, H. G. Sandalidis, and D. Varoutas, "WiMAX on FSO: Outage probability analysis," *IEEE Transactions on Communications*, vol. 60, no. 10, pp. 2789-2795, 2012.

[32] N. Zdravković, M. I. Petkovic, G. T. Djordjevic, and K. Kansanen, "Outage analysis of mixed FSO/WiMAX link," *IEEE Photonics Journal*, vol. 8, no. 1, pp. 1-14, 2016.

[33] G. Keiser, *Optical Fiber Communications*, John Wiley and Sons, Inc., 2003, ch 1, pp. 2-7.

[34] M. Selvi and K. Murugesan, "The performance of orthogonal frequency division multiplexing in the weak turbulence regime of free space optics communication systems," *Journal of Optics*, vol. 14, no. 12, pp. 125401-125406, 2012.

[35] A. N. Stassinakis, H. E. Nistazakis, K. P. Peppas, and G. S. Tombras, "Improving the availability of terrestrial FSO links over log normal atmospheric turbulence channels using dispersive chirped Gaussian pulses," *Optics & Laser Technology*, vol. 54, pp. 329-334, 2013.

[36] G. K. Varotsos, A. N. Stassinakis, *et al*., "Probability of fade estimation for FSO links with time dispersion and turbulence modeled with the gamma–gamma or the IK distribution," *Optik-International Journal for Light and Electron Optics*, vol. 125, no. 24, pp. 7191-7197, 2014.

[37] H. Lu, W. Zhao, and X. Xie, "Analysis of temporal broadening of optical pulses by atmospheric dispersion in laser communication system," *Optics Communications*, vol. 285, no. 13, pp. 3169-3173, 2012.

[38] R. M. Gagliardi, Robert, and S. Karp, *Optical Communications*, New York, Wiley-Interscience, 1976, pp. 445.

[39] W. O. Popoola, Z. Ghassemlooy, J. I. H. Allen, E. Leitgeb, and S. Gao, "Free-space optical communication employing subcarrier modulation and spatial diversity in atmospheric turbulence channel," *IET Optoelectronics*, vol. 2, no. 1, pp. 16-23, 2008.

[40] E. Leitgeb, S. S. Muhammad, C. Chlestil, M. Gebhart, and U. Birnbacher, "Reliability of FSO links in next generation optical networks," in *Proc. 7th International Conference Transparent Optical Networks*, July 2005, vol. 1, pp. 394-401.

[41] E. Leitgeb, M. Gebhart, and U. Birnbacher, "Optical networks, last mile access and applications," *Journal of Optical and Fiber Communications Reports*, vol. 2, no. 1, pp. 56-85, 2005.

[42] E. Leitgeb, M. S. Awan, P. Brandl, T. Plank, C. Capsoni, *et al.*, "Current optical technologies for wireless access," in *Proc. 10th International Conference on Telecommunications*, June 2009, pp. 7-17.

[43] M. S. Awan, E. Leitgeb, F. Nadeem, M. S. Khan, and C. Capsoni, "A new method of predicting continental fog attenuations for terrestrial optical wireless link," in *Proc. Third International Conference on Next Generation Mobile Applications, Services and Technologies*, Sept. 2009, pp. 245-250.

[44] Z. Ghassemlooy, W. O. Popoola, and E. Leitgeb, "Free-space optical communication using subearrier modulation in gamma-gamma atmospheric turbulence," in *Proc. 9th International Conference on Transparent Optical Networks.*, July 2007, vol. 3, pp. 156-160.

[45] X. Zhu and J. M. Kahn, "Free-space optical communication through atmospheric turbulence channels," *IEEE Transactions on Communications*, vol. 50, no. 8, pp. 1293-1300, 2002.

[46] W. Gappmair, S. Hranilovic, and E. Leitgeb, "Performance of PPM on terrestrial FSO links with turbulence and pointing errors," *IEEE Communications Letters*, vol. 14, no. 5, 2010.

[47] X. Zhu and J. M. Kahn, "Performance bounds for coded free-space optical communications through atmospheric turbulence channels," *IEEE Transactions on Communications*, vol. 51, no. 8, pp. 1233-1239, 2003.

[48] D. L. Fried, "Optical heterodyne detection of an atmospherically distorted signal wave front," *Proc. of the IEEE*, vol. 55, no. 1, pp. 57-77, 1967.

[49] A. Laourine, A. Stephenne, and S. Affes, "Estimating the ergodic capacity of log normal channels," *IEEE Commun. Lett.*, vol. 11, no. 7, pp. 568-570, 2007.

[50] S. G. Wilson, M. Brandt-Pearce, Q. Cao, and J. H. Leveque, "Free-space optical MIMO transmission with Q-ary PPM," *IEEE Transactions on Communications*, vol. 53, no. 8, pp. 1402-1412, 2005.

[51] M. M. Ibrahim and A. M. Ibrahim, "Performance analysis of optical receivers with space diversity reception," in *IEEE Proc.-Communications*, vol. 143, no. 6, pp. 369-372, 1996.

[52] A. Katsis, H. E. Nistazakis, and G. S. Tombras, "Bayesian and frequentist estimation of the performance of free space optical channels under weak turbulence conditions," *Journal of the Franklin Institute*, vol. 346, no. 4, pp. 315-327, 2009.

[53] L. C. Andrews and R. L. Phillips, "I–K distribution as a universal propagation model of laser beams in atmospheric turbulence," *JOSA A*, vol. 2, no. 2, pp. 160-163, 1985.

[54] L. C. Andrews and R. L. Phillips, "Mathematical genesis of the I–K distribution for random optical fields," *JOSA A*, vol. 3, no. 11, pp. 1912-1919, 1986.

[55] H. E. Nistazakis, A. D. Tsigopoulos, *et al.*, "Estimation of outage capacity for free space optical Links over IK and K turbulent channels," *Radioengineering*, vol. 20, no. 2, 2011.

[56] B. Epple, "Simplified channel model for simulation of free-space optical communications," *Journal of Optical Communications and Networking*, vol. 2, no. 5, pp. 293-304, 2010.

[57] P. T. Dat, C. B. Naila, P. Liu, K. Wakamori, M. Matsumoto, and K. Tsukamoto, "Next generation free space optics systems for ubiquitous communications," *PIERS Online*, vol. 7, no. 1, pp. 75-80, 2011.

[58] H. G. Sandalidis, "Performance analysis of a laser ground-station-to-satellite link with modulated Gamma-distributed irradiance fluctuations," *J. Opt. Commun. Netw.*, vol. 2, no. 11, pp. 938-943, 2010.

[59] E. Jakeman and P. N. Pusey, "Significance of K distributions in scattering experiments," *Physical Review Letters*, vol. 40, no. 9, pp. 546-550, 1978.

[60] G. Parry, "Measurement of atmospheric turbulence induced intensity fluctuations in a laser beam," *Journal of Modern Optics*, vol. 28, no. 5, pp. 715-728, 1981.

[61] R. L. Phillips and L. C. Andrews, "Measured statistics of laser-light scattering in atmospheric turbulence," *JOSA*, vol. 71, no. 12, pp. 1440-1445, 1981.

[62] R. L. Phillips and L. C. Andrews, "Universal statistical model for irradiance fluctuations in a turbulent medium," *JOSA*, vol. 72, no. 7, pp. 864-870, 1982.

[63] G. R. Osche, "Optical detection theory for laser applications," *Wiley-VCH*, July 2002, p. 424.

[64] A. Garcia-Zambrana, "Error rate performance for STBC in free-space optical communications through strong atmospheric turbulence," *IEEE Communications Letters*, vol. 11, no. 5, 2007.

[65] A. Garcia-Zambrana, B. Castillo-Vázquez, and C. Castillo-Vázquez, "Average capacity of FSO links with transmit laser selection using non-uniform OOK signaling over exponential atmospheric turbulence channels," *Optics Express*, vol. 18, no. 19, pp. 20445-20454, 2010.

[66] H. E. Nistazakis, "A time-diversity scheme for wireless optical links over exponentially modeled turbulence channels," *Optik-International Journal for Light and Electron Optics*, vol. 124, no. 13, pp. 1386-1391, 2013.

[67] H. E. Nistazakis, V. D. Assimakopoulos, and G. S. Tombras, "Performance estimation of free space optical links over negative exponential atmospheric turbulence channels," *OPTIK-International Journal for Light and Electron Optics*, vol. 122, no. 24, pp. 2191-2194, 2011.

[68] W. O. Popoola, Z. Ghassemlooy, and V. Ahmadi, "Performance of sub-carrier modulated free-space optical communication link in negative exponential atmospheric turbulence environment," *International Journal of Autonomous and Adaptive Communications Systems*, vol. 1, no. 3, pp. 342-355, 2008.

[69] M. A. Al-Habash, L. C. Andrews, and R. L. Phillips, "Mathematical model for the irradiance probability density function of a laser beam propagating through turbulent media," *Optical Engineering*, vol. 40, no. 8, pp. 1554-1562, 2001.

[70] L. C. Andrews, R. L. Phillips, C. Y. Hopen, and M. A. Al-Habash, "Theory of optical scintillation," *JOSA A*, vol. 16, no. 6, pp. 1417-1429, 1999.

[71] W. Gappmair and H. E. Nistazakis, "Subcarrier PSK performance in terrestrial FSO links impaired by gamma-gamma fading, pointing errors, and phase noise," *Journal of Lightwave Technology*, vol. 35, no. 9, pp. 1624-1632, 2017.

[72] I. S. Ansari, F. Yilmaz, and M. S. Alouini, "Performance analysis of FSO links over unified Gamma-Gamma turbulence channels," in *Proc. 81st Vehicular Technology Conference (VTC Spring)*, May 2015, pp. 1-5.

[73] H. E. Nistazakis, A. N. Stassinakis, S. Sinanović, W. O. Popoola, and G. S. Tombras, "Performance of quadrature amplitude modulation orthogonal frequency division multiplexing-based free space optical links with non-linear clipping effect over gamma–gamma modelled turbulence channels," *IET Optoelectronics*, vol. 9, no. 5, pp. 269-274, 2015.

[74] W. Gappmair and M. Flohberger, "Error performance of coded FSO links in turbulent atmosphere modeled by gamma-gamma distributions," *IEEE Transactions on Wireless Communications*, vol. 8, no. 5, 2009.

[75] M. Uysal, J. Li, and M. Yu, "Error rate performance analysis of coded free-space optical links over gamma-gamma atmospheric turbulence channels," *IEEE Transactions on Wireless Communications*, vol. 5, no. 6, pp. 1229-1233, 2006.

[76] T. A. Tsiftsis, "Performance of heterodyne wireless optical communication systems over gamma-gamma atmospheric turbulence channels," *Electronics Letters*, vol. 44, no. 5, pp. 372-373, 2008.

[77] E. Bayaki, R. Schober, and R. K. Mallik, "Performance analysis of MIMO free-space optical systems in gamma-gamma fading," *IEEE Transactions on Communications*, vol. 57, no. 11, pp. 3415-3424, 2009.

[78] C. Liu, Y. Yao, Y. Sun, and X. Zhao, "Average capacity for heterodyne FSO communication systems over gamma-gamma turbulence channels with pointing errors," *Electronics Letters*, vol. 46, no. 12, pp. 851-853, 2010.

[79] A. Jurado-Navas, J. M. Garrido-Balsells, J. F. Paris, and A. Puerta-Notario, "A unifying statistical model for atmospheric optical scintillation," in *Numerical Simulations of Physical and Engineering Processes*, 2011, ch. 8, pp. 182-206.

[80] G. Djordjevic, M. Petkovic, A. Cvetkovic, and G. Karagiannidis, "Mixed RF/FSO relaying with outdated channel state information," *IEEE Journal on Selected Areas in Communications*, vol. 33, no. 9, pp. 1935-1948, 2015.

[81] I. S. Ansari, F. Yilmaz, and M. S. Alouini, "Performance analysis of free-space optical links over málaga turbulence channels with pointing errors," *IEEE Transactions on Wireless Communications*, vol. 15, no. 1, pp. 91-102, 2016.

[82] A. Jurado-Navas, J. M. Garrido-Balsells, J. F. Paris, M. Castillo-Vázquez, and A. Puerta-Notario, "Impact of pointing errors on the performance of generalized atmospheric optical channels," *Optics Express*, vol. 20, no. 11, pp. 12550-12562, 2012.

[83] P. Wang, R. Wang, L. Guo, T. Cao, and Y. Yang, "On the performances of relay-aided FSO system over M distribution with pointing errors in presence of various weather conditions," *Optics Communications*, vol. 367, pp. 59-67, 2016.

[84] G. K. Varotsos, H. E. Nistazakis, M. I. Petkovic, G. T. Djordjevic, and G. S. Tombras, "SIMO optical wireless links with nonzero boresight pointing errors over *M* modeled turbulence channels," *Elsevier Optics Communications*, vol. 403, pp. 391-400, 2017.

[85] H. G. Sandalidis, N. D. Chatzidiamantis, and G. K. Karagiannidis, "A tractable model for turbulence-and misalignment-induced fading in optical wireless systems," *IEEE Communications Letters*, vol. 20, no. 9, pp. 1904-1907, 2016.

[86] H. G. Sandalidis, N. D. Chatzidiamantis, G. D. Ntouni, and G. K. Karagiannidis, "Performance of free-space optical communications over a mixture composite irradiance channel," *Electronics Letters*, vol. 53, no. 4, pp. 260-262, 2017.

[87] D. Kedar and S. Arnon, "Urban optical wireless communications networks: The main challenges and possible solutions," *IEEE Commun. Mag.*, vol. 42, no. 5, pp. 2–7, Feb. 2003.

[88] H. G. Sandalidis, T. A. Tsiftsis, G. K. Karagiannidis, and M. Uysal, "BER performance of FSO links over strong atmospheric turbulence channels with pointing errors," *IEEE Communications Letters*, vol. 12, no. 1, pp. 44-46, 2008.

[89] G. T. Djordjevic, M. I. Petkovic, M. Spasic, and D. S. Antic, "Outage capacity of FSO link with pointing errors and link blockage," *Optics Express*, vol. 24, no. 1, pp. 219-230, 2016.

[90] F. Yang, J. Cheng, and T. A. Tsiftsis, "Free-space optical communication with nonzero boresight pointing errors," *IEEE Transactions on Communications*, vol. 62, no. 2, pp. 713-725, 2014.

[91] W. Gappmair, S. Hranilovic, and E. Leitgeb, "OOK performance for terrestrial FSO links in turbulent atmosphere with pointing errors modeled by Hoyt distributions," *IEEE Communications Letters*, vol. 15, no. 8, pp. 875-877, 2011.

[92] I. S. Ansari, M. S. Alouini, and J. Cheng, "Ergodic capacity analysis of free-space optical links with nonzero boresight pointing errors," *IEEE Transactions on Wireless Communications*, vol. 14, no. 8, pp. 4248-4264, 2015.

[93] H. AlQuwaiee, H. C. Yang, and M. S. Alouini, "On the asymptotic capacity of dual-aperture FSO systems with generalized pointing error model," *IEEE Transactions on Wireless Communications*, vol. 15, no. 9, pp. 6502-6512, 2016.

[94] R. Boluda-Ruiz, A. García-Zambrana, C. Castillo-Vázquez, and B. Castillo-Vázquez, "Novel approximation of misalignment fading modeled by Beckmann distribution on free-space optical links," *Optics Express*, vol. 24, no. 20, pp. 22635-22649, 2016.

[95] R. Boluda-Ruiz, A. García-Zambrana, B. Castillo-Vázquez, and C. Castillo-Vázquez, "Impact of nonzero boresight pointing error on ergodic capacity of MIMO FSO communication systems," *Optics Express*, vol. 24, no. 4, pp. 3513-3534, 2016.

[96] S. William and I. Djordjevic, "OFDM in Free-Space Optical communication Systems," in *OFDM for Optical Communications*, Academic Press, 2009, ch. 10, pp. 351-384.

[97] W. Huang, J. Takayanagi, T. Sakanaka, and M. Nakagawa, "Atmospheric optical communication system using subcarrier PSK modulation," *IEICE Transactions on Communications*, vol. 76, no. 9, pp. 1169-1177, 1993.

[98] M. Z. Hassan, M. J. Hossain, J. Cheng, and V. C. Leung, "Subcarrier intensity modulated optical wireless communications: A survey from communication theory perspective," *ZTE Communications*, vol. 2, pp. 1-11, 2016.

[99] X. Song and J. Cheng, "Optical communication using subcarrier intensity modulation in strong atmospheric turbulence," *Journal of Lightwave Technology*, vol. 30, no. 22, pp. 3484-3493, 2012.

[100] X. Song, F. Yang, and J. Cheng, "Subcarrier intensity modulated optical wireless communications in atmospheric turbulence with pointing errors," *Journal of Optical Communications and Networking*, vol. 5, no. 4, pp. 349-358, 2013.

[101] J. Li, J. Q. Liu, and D. P. Taylor, "Optical communication using subcarrier PSK intensity modulation through atmospheric turbulence channels," *IEEE Transactions on Communications*, vol. 5, no. 8, pp. 1598-1606, 2007.

[102] M. Petkovic and G. T. Djordjevic, "SEP analysis of FSO system employing SIM-MPSK with noisy phase reference," in *Proc. 4th International Workshop on Optical Wireless Communications*, Sept. 2015, pp. 46-50.

[103] B. J. Dixon, R. D. Pollard, and S. Iezekiel, "Orthogonal frequency-division multiplexing in wireless communication systems with multimode fiber feeds," *IEEE Transactions on Microwave Theory and Techniques*, vol. 49, no. 8, pp. 1404-1409, 2001.

[104] J. Armstrong, "OFDM for optical communications," *Journal of Lightwave Technology*, vol. 27, no. 3, pp. 189-204, 2009.

[105] L. Chen, B. Krongold, and J. Evans, "Performance evaluation of optical OFDM systems with nonlinear clipping distortion," in *Proc. International Conference on Communications*, June 2009, pp. 1-5.

[106] Y. Wang, D. Wang, and J. Ma, "Performance analysis of multihop coherent OFDM free-space optical communication systems," *Optics Communications*, vol. 376, pp. 35-40, 2016.

[107] Y. Wang, D. Wang, and J. Ma, "On the performance of coherent OFDM systems in free-space optical communications," *IEEE Photonics Journal*, vol. 7, no. 4, pp. 1-10, 2015.

[108] K. Tsukamoto, T. Higashino, T. Nakamura, K. Takahashi, Y. Aburakawa, S. Komaki, and K. Omae, "Development of radio on free space optics system for ubiquitous wireless," *PIERS Online*, vol. 4, no. 1, pp. 96-100, 2008.

[109] D. Tsonev, S. Sinanovic, and H. Haas, "Novel unipolar orthogonal frequency division multiplexing (U-OFDM) for optical wireless," in *Proc. 75th Vehicular Technology Conference (VTC Spring)*, May 2012, pp. 1-5.

[110] D. Tsonev, S. Sinanovic, and H. Haas, "Complete modeling of nonlinear distortion in OFDM-based optical wireless communication," *Journal of Lightwave Technology*, vol. 31, no. 18, pp. 3064-3076, 2013.

[111] S. Dimitrov, S. Sinanovic, and H. Haas, "Clipping noise in OFDM-based optical wireless communication systems," *IEEE Transactions on Communications*, vol. 60, no. 4, pp. 1072-1081, 2012.

[112] W. Shieh and C. Athaudage, "Coherent optical orthogonal frequency division multiplexing," *Electronics Letters*, vol. 42, no. 10, pp. 587-589, 2006.

[113] N. D. Chatzidiamantis, D. S. Michalopoulos, E. E. Kriezis, G. K. Karagiannidis, and R. Schober, "Relay selection protocols for relay-assisted free-space optical systems," *Journal of Optical Communications and Networking*, vol. 5, no. 1, pp. 92-103, 2013.

[114] M. A. Kashani, M. Safari, and M. Uysal, "Optimal relay placement and diversity analysis of relay-assisted free-space optical communication systems," *Journal of Optical Communications and Networking*, vol. 5, no. 1, pp. 37-47, 2013.

[115] T. A. Tsiftsis, H. G. Sandalidis, G. K. Karagiannidis, and N. C. Sagias, "Multihop free-space optical communications over strong turbulence channels," in *Proc. International Conference on Communications*, June 2006, vol. 6, pp. 2755-2759.

[116] K. P. Peppas, A. N. Stassinakis, H. E. Nistazakis, and G. S. Tombras, "Capacity analysis of dual amplify-and-forward relayed free-space optical communication systems over turbulence channels with pointing errors," *Journal of Optical Communications and Networking*, vol. 5, no. 9, pp. 1032-1042, 2013.

[117] K. Prabu and D. S. Kumar, "Outage analysis of relay-assisted BPSK-SIM based FSO systems over strong atmospheric turbulence with pointing errors," *International Journal of Computer and Communication Engineering*, vol. 3, no. 5, pp. 317-320, 2014.

[118] A. S. Acampora and S. V. Krishnamurthy, "A broadband wireless access network based on mesh-connected free-space optical links," *IEEE Personal Communications*, vol. 6, no. 5, pp. 62-65, 1999.

[119] J. Akella, M. Yuksel, and S. Kalyanaraman, "Error analysis of multi-hop free-space optical communication," in *Proc. IEEE International Conference on Communications*, May 2005, vol. 3, pp. 1777-1781.

[120] G. K. Karagiannidis, T. A. Tsiftsis, and H. G. Sandalidis, "Outage probability of relayed free space optical communication systems," *Electronics Letters*, vol. 42, no. 17, pp. 994-996, 2006.

[121] M. Safari and M. Uysal, "Relay-assisted free-space optical communication," *IEEE Transactions on Wireless Communications*, vol. 7, no. 12, pp. 5441-5449, 2008.

[122] H. E. Nistazakis, M. P. Ninos, A. D. Tsigopoulos, D. A. Zervos, and G. S. Tombras, "Performance study of terrestrial multi-hop OFDM FSO communication systems with pointing errors over turbulence channels," *Journal of Modern Optics*, vol. 63, no. 14, pp. 1403-1413, 2016.

[123] The Wolfarm Functions Site. (2008). [Online]. Available: http:/functions.wolfarm.com

[124] V. S. Adamchik and O. I. Marichev, "The algorithm for calculating integrals of hypergeometric type functions and its realization in reduce system," in *Proc. International Symposium on Symbolic and Algebraic Computation*, July 1990, pp. 212-224.

[125] J. G. Proakis, "Optimum receivers for the AWGN channels," in *Digital Communications, 4th ed*., New York, McGraw-Hill, 2001, ch. 5, pp. 278-282.

[126] Q. Zhang, J. Cheng, and G. K. Karagiannidis, "Block error rate of optical wireless communication systems over atmospheric turbulence channels," *IET Communications*, vol. 8, no. 5, pp. 616-625, 2014.